Spin and Orbital Ground State of Co in Cobalt Phthalocyanine

T. Kroll,*,† V. Yu. Aristov,†,‡ O. V. Molodtsova,† Yu. A. Ossipyan,‡ D. V. Vyalikh,¶ B. Büchner,† and M. Knupfer†

IFW Dresden, P.O. Box 270016, D-01171 Dresden, Germany, Institute of Solid State Physics, Russian Academy of Sciences, Chernogolovka, Moscow distr. 142432, Russia, and Institute of Solid State Physics, TU Dresden, D-01069 Dresden, Germany

Received: April 1, 2009; Revised Manuscript Received: June 5, 2009

The 3d orbital ground state of transition-metal ions that are incorporated in a molecular matrix determines the total spin of the transition-metal ion as well as the spin anisotropy and thus the essential magnetic properties of the corresponding molecule. However, there is little known to date on the exact 3d ground state of many molecular systems, including quite complex molecular magnets as well as relatively simple systems such as, for instance, cobalt phthalocyanine (CoPc). For the latter, there are contradictory theoretical predictions with respect to the occupation of the various Co 3d electronic levels. We demonstrate that polarization-dependent X-ray absorption spectroscopy in combination with a simulation of the spectra is able to shed a brighter light on the spin and orbital ground state of the transition-metal ion in CoPc. Our results reveal a temperature-dependent ground state and emphasize the importance of taking 3d correlation effects properly into account.

Introduction

In general, the electronic structures of transition-metal phthalocyanine (MPc) complexes offer valuable insight into the interaction of the metal ion with its surrounding. Therefore, they can be regarded as a simple model compound for the investigation of the electronic properties of many other transition-metal-containing materials, among them, many molecular magnetic complexes. In fact, MnPc has been referred to as a typical example of a molecular magnet.[1] Surprisingly, despite a large number of experimental and theoretical studies in the last decades, essential details of the electronic structure of MPc's remained unclear. This is also true for CoPc, the subject of our study in this contribution. In particular, there is no consensus on the 3d orbital ground state of Co in CoPc, as outlined below, which, for example, raises the question of how to microscopically rationalize more complicated molecular magnets and their chemical and physical properties when this has not been achieved for the rather simple CoPc molecule. We emphasize that the 3d orbital ground state determines the total spin of the transition-metal ion as well as the spin anisotropy, that is, essential quantities for the understanding of the magnetic behavior of the molecule. Moreover, an unambiguous experimental determination is important in order to test and develop theoretical models and calculations.

In Figure 1, a single CoPc molecule is shown. These complexes consist of a phthalocyanine (Pc) ring that incorporates a transition-metal ion in its center. In fact, almost every metal in the periodic table can be combined with the Pc molecule, and most of these complexes show a very high thermal and chemical stability. Their electronic and, in particular, magnetic properties are determined by the valence and spin state of the transition-metal ion. Therefore, these properties can be varied by substituting the transition-metal ion or doping the system with electrons or holes.

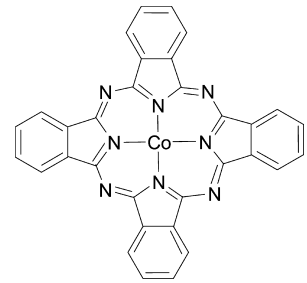

Figure 1. Scheme of the chemical structure of a cobalt phthalocyanine molecule. The local symmetry around the central transition-metal ion is tetragonal (D_{4h} symmetry), where the molecule's z-axis points along the normal of the molecular plane.

As illustrated in Figure 1, the CoPc molecule has a tetragonal symmetry with its z-axis oriented normal to the molecular plane. Even though the crystal structure of CoPc indicates that the molecule is not perfectly planar,[2,3] its local symmetry is surely D_{4h} in solution[4] and in the gas phase.[5] It is therefore reasonable to assume D_{4h} symmetry for CoPc molecules in thin films too. In this context, it is an important point that also in the solid state, the electronic structure is predominantly determined by the electronic structure of a single molecule, as shown for NiPc.[6] Some theoretical descriptions using calculations of a single molecule have been successfully used in the past to describe properties of MPC films.[7−9]

Placing a transition-metal ion in a molecule results in a splitting of the formerly degenerate transition-metal 3d bands. This splitting depends on the symmetry of the surrounding. An octahedral environment (O_h symmetry) causes a splitting into two levels with e_g and t_{2g} symmetry. Going to tetragonal symmetry, the levels split further (see Figure 2). The order of their corresponding energies depends on the strength and type of the distortion, as well as on hybridization effects.[10,11]

For many MPc's, there exists no consistent picture of the electronic ground state. In CoPc, the divalent Co(II) ion is a $3d^7$ system with a possible $S = 1/2$ low-spin or $S = 3/2$ high-spin configuration. Charge density studies as well as theoretical

* To whom correspondence should be addressed. E-mail: t.kroll@ifw-dresden.de.
† IFW Dresden.
‡ Russian Academy of Sciences.
¶ TU Dresden.

10.1021/jp903001v CCC: $40.75
Published on Web 07/10/2009

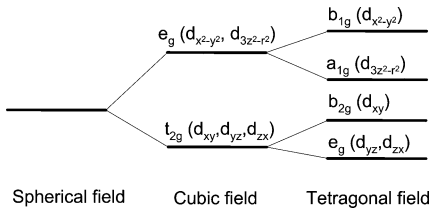

Figure 2. Sketch of the energy splitting due to a cubic and tetragonal field. In the tetragonal case, a formerly cubic octahedron has been elongated, which leads to such an energy scheme. In fact, including covalency, the energy level may have a different ordering, as is the case for CoPc.

calculations such as density functional theory (DFT) calculations hint toward a low-spin $S = 1/2$ situation.[12−17] In such a configuration, the b_{1g} ($3d_{x^2-y^2}$) orbital is predicted to be empty, whereas the $3d_{xy}$, $3d_{xz,yz}$ and $3d_{3z^2-r^2}$ orbitals are close in energy. All interpretations of experimental and theoretical investigations coincide in the conclusion that the $3d_{x^2-y^2}$ orbital is completely empty, but there is substantial disagreement in the character of the half-filled orbital. Calculations based on DFT find the Co $3d_{3z^2-r^2}$ orbital to be half filled and the $3d_{xz,yz}$ orbitals fully occupied,[15−17] whereas other DFT calculations find an inverted situation with the Co $3d_{3z^2-r^2}$ orbital being fully occupied and $3d_{xz,yz}$ orbitals containing one hole.[13,14] Note that the latter situation would cause an instability of the phthalocyanine molecule with respect to a Jahn−Teller-like distortion, which would lift the degeneracy of the e_g level.[18,19] Another different ground state has been inferred experimentally from charge density studies.[12] There, a strongly anisotropic orbital population was observed, with effectively 4.9(1) electrons in the Co 3d shell, $(3d_{x^2-y^2})^{0.0}(3d_{zx,yz})^{2.4}(3d_{3z^2-r^2})^{0.8}(3d_{xy})^{1.8}(4p_z)^{1.1}(4\,p_{x,y})^{1.4}$. Note that a population of Co 4p states is also possible via a back-donating process from the ligands.[20−22] The above-described picture of a $S = 1/2$ $3d^7$ configuration of the Co 3d states finds support from electron paramagnetic resonance (EPR) and susceptibility measurements, which provide evidence for an unpaired electron in the $3d_{3z^2-r^2}$ orbital.[23]

In this article, we present the interpretation of data from X-ray absorption spectroscopy experiments on CoPc molecules. For a detailed investigation of the ground-state electronic structure, X-ray absorption spectroscopy (XAS) is a powerful method since one directly probes the unoccupied states near the chemical potential. Importantly, XAS is also sensitive to valencey, spin state, and orbital orientation, which has already been used to unravel the orbital and spin state of inorganic cobalt compounds.[24−27] Together with a theoretical description, we are able to shed a brighter light on the electronic ground and excited state configurations of the transition-metal Co ion in CoPc. Furthermore, we find the ground and first excited state in close proximity in energy, which indicates a temperature dependence of the resulting absorption spectra as well as magnetic properties.

Experimental Methods

When MPc molecules crystallize in a solid state, the planar MPc molecules are arranged as weakly coupled one-dimensional stacks resulting in strongly anisotropic physical properties such as quasi one-dimensional Ising chains.[5,28] Within the stacks, the MPc molecules are tilted toward each other. The neighboring stack has the same tilting angle but is oriented in the opposite direction.

Such a crystallographic structure is somewhat unfavorable for experiments using polarized light since, due to the tilting of the MPc molecular stacks, the polarization information is partially lost, depending on the size of the angle. A very different ordering is observed for MPc thin films on a, for example, gold single-crystal substrate. In this case, the MPc molecules lie flat on the surface with a well-defined main axis for all molecules,[29,30] that is, the sample surface normal is oriented parallel to the molecular z-axis. The distance between MPc molecules in thin films is comparable to the crystal lattice parameters,[31,32] so that the internal parameters that determine the electronic structure remain unchanged. Furthermore, using a metallic gold substrate has the advantage of forming well-defined interfaces since the gold substrate does not interact with the MPc layers,[33,34] besides the direct layers which build the interface itself. This situation is very favorable for optical methods like X-ray absorption spectroscopy since, in this case, a polarization dependence can be observed which increases the reliability of the interpretation of the spectra.

As described in detail in ref 35, a CoPc 7 nm thin film has been grown in situ on a clean Au(001) single crystal. The chosen thickness is large enough to minimize contributions from the gold substrate and sufficiently small to keep flat-lying molecules, and this was verified by photoemission studies. Polarization-dependent X-ray absorption at the C and N K-edge and low-energy electron diffraction (LEED) revealed that the CoPc molecules were indeed lying flat on the single-crystal Au substrate for the investigated film. Furthermore, the sample has been measured directly after its preparation in order to avoid contamination on the surface.

Polarization-dependent X-ray absorption spectroscopy studies of such films at the Co $L_{2,3}$-edge have been performed at the Russian−German beamline of the synchrotron radiation source Bessy II, Berlin. The resolution was set to 150 meV at 780 eV of photon energy, and the percentage of the linear polarization was 98%. The absorption spectra were recorded in the total electron yield mode and normalized to the incident photon flux. According to the dipole selection rules, the Co $L_{2,3}$ excitations as probed by these experiments, correspond to excitations of Co 2p core-level electrons into unoccupied Co 3d electronic states. Upon variation of the energy of the incident light and its polarization, different Co 3d orbitals can be probed.[36−38] For polarization-dependent measurements, the sample was rotated such that the direction of incident photons and the sample surface normal (i.e., the z-axis of a molecule) enclose an angle Θ between 6 and 76° (cf. inset in Figure 3). In order to rule out radiation damage effects, normal incident spectra were repeated after the whole run. The data could be well reproduced, and sample damages could be excluded.

Computational Details

A direct interpretation of the data is difficult since besides the one-electron on-site energies, also Coulomb and exchange interactions and spin−orbit coupling have to be taken into account[10] in the initial state, leaving out hybridization effects for the moment. In the X-ray absorption excited state, a 2p core hole has been created, which interacts with valence electrons via Coulomb interactions too. Its energy scale is in the range of a few eV and leads to an additional multiplet splitting.[38,43]

Intra-atomic multiplet calculations were performed using the atomic theory developed by Cowan and the crystal field (i.e., symmetry) interactions described by Butler.[11,44] This approach includes both electronic Coulomb interactions and spin−orbit coupling for each subshell.[36,38] The calculations have been done for divalent Co^{2+} ($3d^7$) in a tetragonal environment (D_{4h} symmetry). To simulate the spectra, the Slater−Condon parameters (F_i and G_i) were reduced of their Hartree−Fock-

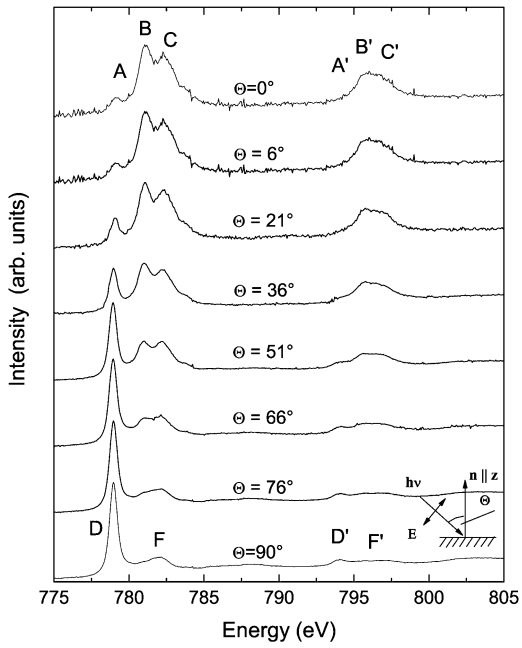

Figure 3. Polarization-dependent NEXAFS data of flat-lying CoPc molecules on a single-crystal Au substrate. The *z*-axis of the molecules points in the direction of the surface normal **n**, and Θ gives the angle between the surface normal **n** and the direction of the incident beam. The electric field vector **E** of the incident beam is linearly polarized perpendicular to the direction of propagation. At Θ = 0°, the incident beam is polarized in-plane to the *x*,*y*-plane of CoPc, that is, perpendicular to the molecular *z*-axis, and at Θ = 90°, it is out-of-plane, that is, parallel to the molecular *z*-axis. The spectra for Θ = 0 and 90° were calculated from the spectra of Θ = 6 and 76°.[39]

calculated values to account for the overestimation of electron−electron repulsion found in calculations of the free ion.

Covalency leads to a screening of the core−hole effect. This effect has been taken into account by partially reducing the Slater−Condon parameters compared to their value in a free ion.[36,41,42] Therefore, the only fitting parameters were the crystal field values for tetragonal symmetry (D_{4h}) *Dq*, *Ds*, and *Dt*,[10,11] as well as a reduction of the Slater−Condon parameters.

Results and Discussion

In Figure 3, experimental XAS data at room temperature at the Co $L_{2,3}$-edge of CoPc are shown for different sample orientations in order to gain polarization-dependent information.

The XAS spectra are divided into two main regions, the Co L_3- and L_2-edges, which are separated by ∼15 eV. These refer to the spin−orbit coupling of the 2p core hole of the excited state with $j = 3/2$ (L_3) and $j = 1/2$ (L_2), where the L_3-edge appears at lower energies. In Figure 3, from top to bottom, the angle Θ between the incident light and the surface normal (*z*-axis) varies from 0 to 90°, where a situation of 0° corresponds to a polarization perpendicular to the *z*-axis and 90° corresponds to a polarization parallel to the *z*-axis. The two extreme cases Θ = 0 and 90° have been extracted from the spectra of Θ = 6 and 76°.[39]

At higher energies ∼788 and ∼803 eV, weak and broad peaks appear, which are strongest for the electric light vector being oriented parallel to the molecular *z*-axis. In ref 40, it has been stated for CuPc that the 4s (a_{1g}) orbital is weakly hybridized with the out-of-plane $3d_{3z^2-r^2}$ orbital. In the XAS spectra of CuPc, this hybridization leads to a polarization-dependent (weak) peak about 8 eV above the main absorption peak. Therefore, we assume that the features at ∼788 and ∼803 eV in CoPc have the same origin.

As can be seen in this figure, in each of the two edges, there are two main regions with a contrary polarization-dependent behavior. Here, we focus the discussion on the L_3 absorption edge. The first peak at ∼779 eV (peak A for Θ = 0° ($E \perp z$) and peak D for Θ = 90° ($E \parallel z$)) increases with increasing Θ, whereas the two peaks at around 781 and 782.3 eV (peaks B and C and peak F for Θ = 0 and 90°, respectively) decrease with increasing Θ.

When simulating the spectra using intra-atomic multiplet calculations as described in the Computational Details section, special attention has been paid to certain criteria in the experimental spectra, besides the overall agreement. (i) The small peak at 782 eV for $E \parallel z$ does not originate from a (partial) misalignment of the sample but is a real feature which has to be found in the theoretical spectra too. (ii) The intensity ratio between the L_3- and L_2-edges is determined by the spin state as well as by 3d spin−orbit coupling[45] and has to be reproduced.

After an extensive search over a huge parameter range, no satisfying agreement between experimental and theoretical spectra could be found when using only the ground state of each parameter set for modeling the theoretical spectra and neglecting all excited states for a description of the undisturbed system. Since the experimental spectra have been taken at room temperature, first excited states may play an important role if the energy difference is in the range of up to about 50 meV, and indeed, when taking the first excited state into account (the second excited state is far off), the experimental spectra can be well described. It turned out that two parameter sets describe the data equally well, even though there are slight differences in the spectra. One parameter set leads to a "configuration I" with crystal field parameters $Dq = 0.23$, $Ds = 0.82$, and $Dt = 0.16$ and a reduction of the Slater−Condon parameters to 65% of their free ion values. "Configuration II" accounts to the second parameter set $Dq = 0.28$, $Ds = 0.58$, and $Dt = 0.27$ and to 70% reduced Slater−Condon parameters. In Figure 4, these spectra are shown for both configurations I and II (left and right) and both polarizations (top and bottom) calculated for 300 K and taking all interactions into account.

Earlier calculations by Thole et al.[7] during the late 1980s for FePc also point toward a temperature dependence of the X-ray absorption spectra very similar to what is presented here. Although different from CoPc, they also found a spin-mixed ground state in FePc that still has to be verified experimentally.

From earlier investigations of CoPc, such as charge density studies and DFT calculations, it is known that the spin state is $S = 1/2$ and the $3d_{x^2-y^2}$ orbital is highest in energy and therefore completely empty.[12−17] Such a situation has been found for both configurations, which confirms a low spin state of $S = 1/2$ for CoPc. However, the orbital occupation of the third hole strongly depends on the chosen parameter set. The dependence of the orbital occupation shall therefore be discussed in more detail in the following.

In Figure 5, the electronic structure of the Co^{2+} ion for both parameter sets has been sketched. The top part refers to the parameter set that relates to configuration I, and the bottom part refers to the parameter set that relates to configuration II.[46] The left column displays the results where only the crystal field influence is included, that is, one electron picture (configurations Ia and IIa), in the middle column, also Coulomb and exchange interactions have been taken into account (configurations Ib and IIb), and the right column shows the results of the full Hamiltonian that also respects spin−orbit coupling (configura-

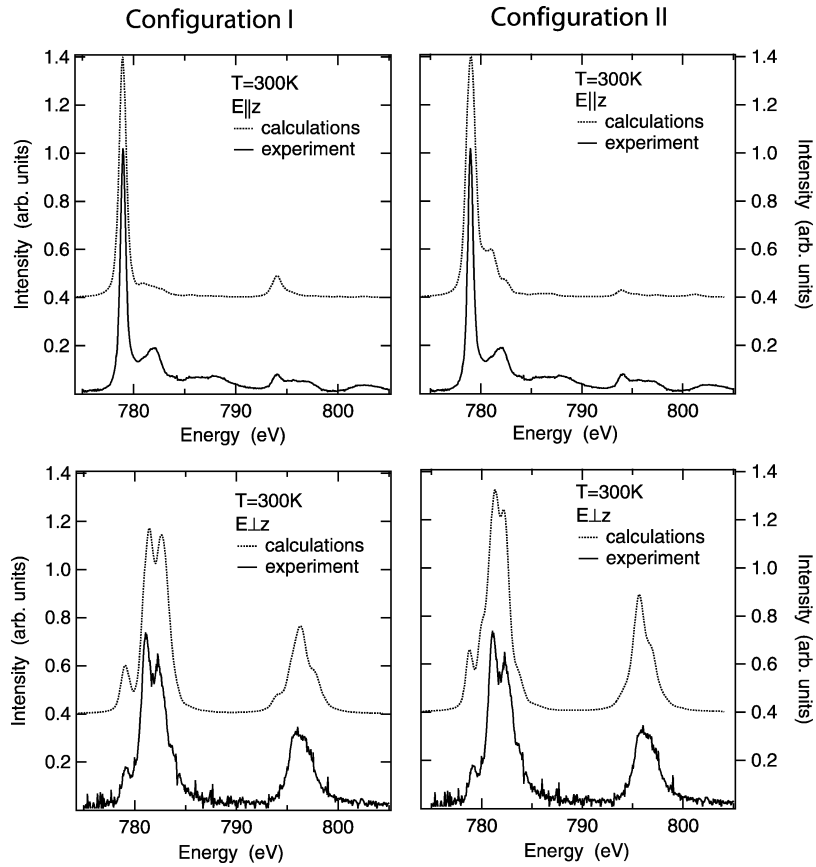

Figure 4. Comparison of multiplet calculations and experimental data between both configurations I and II (left and right; see Figure 5) and both polarizations (top and bottom). For the experimental data, the extrapolated spectra $\Theta = 0$ ($E \perp z$) and 90° ($E \parallel z$) have been used. For a room-temperature description, the two lowest-energy states have been Boltzmann weighted. See the text for a configuration description.

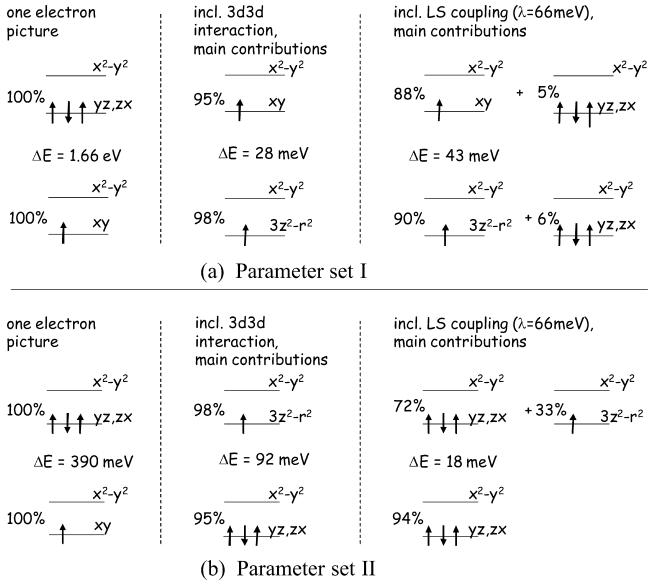

Figure 5. A sketch of the electronic structure as calculated for configurations I and II.[46] Only the two highest-energy levels are shown since the lower ones are fully occupied. All columns show the electronic configuration of the ground and first excited state and the energy separation between them. The left column displays the results where only the crystal field influence is included (i.e., the one-electron picture); in the middle column, also Coulomb and exchange interactions have been taken into account, and the right column shows the results of the full Hamiltonian that also respects spin−orbit coupling.

tions Ic and IIc). Note that only the two highest energy levels are shown since the lower ones are fully occupied. Naturally, the most realistic model is described by the full Hamiltonian (right column), while the left and middle columns act as examples to illustrate the influence of all parameters in these calculations. Therefore, configurations I and II refer to configurations Ic and IIc.

For both crystal fields that have been used for the two configurations Ia and IIa, the one electron picture (i.e., taking only crystal field effects into account) finds the third hole in the *xy* 3d orbital in the ground state, whereas the first excited state is far off (1.66 and 0.39 eV for configurations Ia and IIa, respectively) and contains its third hole in the *yz*,*zx* orbitals (see Figure 5, left column).

This situation changes dramatically when also taking Coulomb and exchange interaction between the 3d electrons into account (i.e., switching on the Slater−Condon parameters). In this case, differences between both configurations Ib and IIb appear, and remarkably enough, the energy difference between the ground and first excited state becomes small (less than 100 meV, middle column). For configuration Ib, the ground state is built by a configuration that finds the third hole to 98% in the $3z^2-r^2$ orbital, whereas its first excited state is just 28 meV higher in energy with the third hole mainly in the *xy* orbital (95%). Note that all contributions with less than 2% importance have been neglected here for the sake of clarity. A different situation has been found for configuration IIb. Here, the ground state consists of a configuration with the third hole in the *yz*,*zx* orbitals (95%), with the first excited state 92 meV away and a hole in the $3z^2-r^2$ orbital (98%).

When also taking spin−orbit coupling into account, the overall picture becomes more complicated but does not change dramatically any more (right column). With the spi−orbit ζ_{3d}

parameters $\zeta = 66$ and 82 meV for the ground and excited state, respectively, the ground state of the first configuration Ic finds its third hole to 90% in the $3z^2-r^2$ orbital and to 6% in the *yz*,*zx* orbitals. At 43 meV above, we find an *xy* (88%) and *yz*,*zx* (5%) excited state. After including LS-coupling, the changes from configuration IIb to IIc are stronger. The ground state consists mainly of basis functions with a hole in the *yz*,*zx* orbitals, where the excited state has its main contribution by the third hole also in the *yz*,*zx* orbitals (72%), together with a large amount of $3z^2-r^2$ (33%) holes.

Note that for every eigenvalue, its eigenvector gives the weighted importance of all contributions to that eigenvalue. Therefore, only the appearance of holes in certain orbitals can be calculated but not the energy separation between orbitals as in the one-electron picture.

The existence of a small energy gap between the ground and first excited state leads to a temperature dependence of the electronic structure of Co in CoPc. This may also be a possible explanation for the different interpretations arising from DFT calculations.

In order to distinguish between the two proposed configurations (i.e., configurations Ic and IIc) and determine the correct one, temperature-dependent measurements are necessary. In X-ray absorption spectroscopy, the differences in the electronic structure for the two configurations would have an influence in the shape of the spectra too. This becomes clear when looking at the various spectra that are obtained from taking either the ground state or the first excited state as the initial state in an XAS experiment. As it has been explained above, in X-ray absorption spectroscopy, an electron is excited from a core level into an unoccupied state. Naturally, the shape of the correlated spectra depends strongly on the electronic structure of the initial state.

In Figure 6, calculated X-ray absorption spectra for different initial states are shown. The left column displays the spectra in which the ground state has been taken as the initial state, whereas for the right column, the first excited state has been taken as the initial state. When comparing these spectra with the Boltzmann-weighted 300 K spectra in Figure 4, a clear temperature dependence is predicted. Unfortunately, the ground-state spectra (left column) appear very similar in their overall shape for both configurations (Figure 6a and b), which makes it difficult to distinguish between them at low temperatures. Nevertheless, the spectra with the first excited state taken as the initial state are very different from each other. Especially for a polarization of the incoming light parallel to the molecular *z*-axis, the orbital occupation is completely different for the two configurations (cf. Figure 5 right column). Since configuration I has its third hole in the first excited state mainly in an *xy* orbital, there is almost no intensity for the electric field vector parallel to the *z*-axis (Figure 6a top right). Therefore, the absorption intensity and spectral shape for $E \parallel z$ should change with temperature for configuration I but should remain almost constant with temperature for that polarization for configuration II.

At room temperature, both the ground and first excited state are present. Therefore, different states are probed when changing the polarization, as shown in Figures 5 and 6. While in configuration II the ground and first excited states are very similar, they are different for configuration I. This leads to a situation in which the low-energy peak (which corresponds to D and A in the experimental data of Figure 3) shifts slightly upward in energy when changing the polarization from $E \parallel z$ to $E \perp z$ for configuration I but does not shift for configuration II.

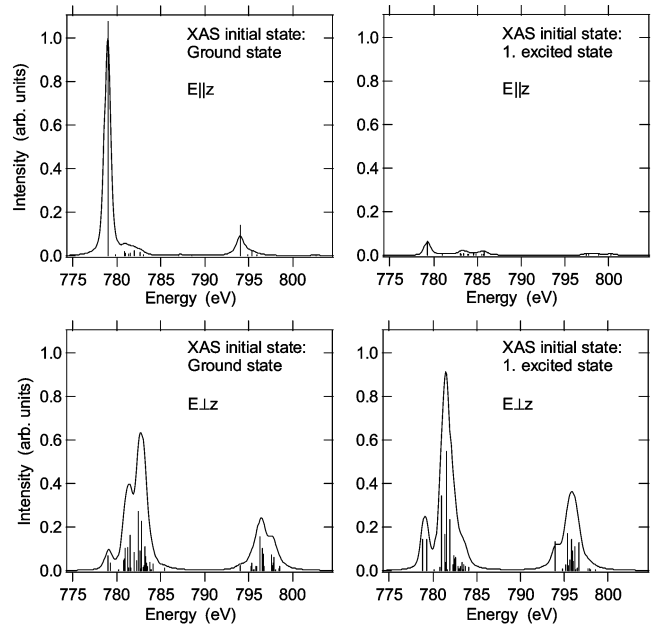

Figure 6. Calculated XAS spectra for different initial states for configurations I and II [(a) and (b), respectively] and polarizations (top and bottom of the two subfigures). The left column displays spectra where the ground state has been taken as the initial state of the absorption process, and the right column shows spectra with the first excited state taken as the initial state.

When comparing this to the experimental data, a slight shift of peak D to higher energies occurs when changing the polarization (peak A). From this observation, an orbital ordering as that found for configuration I may be the most appropriate one. In order to clearly distinguish between these two configurations and unambiguously determine the electronic ground-state configuration of CoPc, temperature-dependent XAS and temperature-dependent X-ray magnetic circular dichroism (XMCD) experiments should be performed.

Summary

In summary, from polarization-dependent X-ray absorption spectroscopy measurements together with intra-atomic multiplet

calculations, predictions for the electronic structure of CoPc molecules could be made. For both possible configurations found, the ground and first excited state are close in energy, so that a mixture of both is present at room temperature. The close proximity in energy of these states as well as the strong influence of Coulomb and exchange interactions and spin−orbit coupling on the electronic structure could be the reason for the disagreement of earlier predictions found by DFT calculations.[12−17] Our data analysis demonstrates the strength of X-ray absorption spectroscopy in combination with a simulation of the spectra to unravel further information on the spin and orbital ground state of transition-metal ions in molecular complexes, which represents an inevitable step toward a complete understanding of their electronic and magnetic properties.

We are able to reduce the number of possible configurations describing the ground state of CoPc to two. In order to distinguish between these two configurations as shown in Figure 5, temperature-dependent measurements are highly desirable. Especially, temperature-dependent X-ray absorption spectroscopy experiments are favorable since a different temperature dependence of the spectra is predicted for the two configurations.

Acknowledgment. We are grateful to R. Hübel, S. Leger, and R. Schönfelder for technical assistance. We also thank F.M.F. de Groot for fruitful discussions and advice. This investigation was supported by the SMWK, the DFG (SFB 463, KN 393/10-1), and the RFBR (Grant Number 08-02-1170). T.K. has been financed by the DFG Project KR 3611/1-1.

References and Notes

(1) Kahn, O. *Molecular Magnetism*; VCH Publishers: New York, 1993; p 323.
(2) Kirner, J. F.; Dow, W.; Scheidt, W. R. *Inorg. Chem.* **1976**, *15*, 1685.
(3) Mason, R.; Williams, G. A.; Fielding, P. E. J. *J. Chem. Soc., Dalton Trans.* **1979**, 676.
(4) Kahl, J. L.; Faulkner, L. R.; Dwarakanath, K.; Tachiwaka, H. J. *J. Am. Chem. Soc.* **1986**, *108*, 5434.
(5) Ruan, C.-Y.; Mastryukov, V.; Fink, M. J. *J. Chem. Phys.,* **1999**, *111*, 3035.
(6) Bialek, B.; Kim, I. G.; Lee, J. I. *Synth. Met.* **2002**, *129*, 151.
(7) Thole, B. T.; van der Laan, G.; Butler, P. H. *Chem. Phys. Lett.* **1988**, *149*, 295.
(8) Rosa, A.; Baerends, E. J. *Inorg. Chem.* **1994**, *33*, 584.
(9) Mirone, A.; Sacchi, M.; Gota, S. *Phys. Rev. B* **2000**, *61*, 13–540.
(10) Ballhausen, C. J. *Ligand Field Theory*; McGraw-Hill Book Company: New York, 1962.
(11) Butler, P. H. *Point Group Symmetry, Applications, Methods and Tables*; Plenum: New York, 1962.
(12) Figgis, B. N.; Kucharski, E. S.; Reynolds, P. A. *J. Am. Chem. Soc.* **1989**, *111*, 1683.
(13) Liang, X. L.; Flares, S.; Ellis, D. E.; Hoffman, B. M.; Musselman, R. L. *J. Chem. Phys.* **1991**, *95*, 403.
(14) Liao, M.-S.; Scheiner, S. *J. Chem. Phys.* **2001**, *114*, 9789.
(15) Reynolds, P. A.; Figgis, B. N. *Inorg. Chem.* **1991**, *30*, 2294.
(16) Rosa, A.; Baerends, E. J. *Inorg. Chem.* **1992**, *31*, 4717.
(17) Bialek, B.; Kim, I. G.; Lee, J. I. *Thin Solid Films* **2006**, *513*, 110.
(18) Tosatti, E.; Fabrizio, M.; Tóbik, J.; Santoro, G. E. *Phys. Rev. Lett.* **2004**, *93*, 117002.
(19) Tóbik, J.; Tosatti, E. *J. Mol. Struct.* **2007**, *838*, 112.
(20) Dewar, M. J. S. *Bull. Soc. Chim. Fr.* **1951**, *18*, C71−C79.
(21) Chatt, J.; Duncanson, L. A. *J. Chem. Soc.* **1953**, 2939–2947.
(22) Frenking, G. J. *Organomet. Chem.* **2001**, *635*, 9–23.
(23) Janczak, J.; Kubuak, R. *Inorg. Chim. Acta* **2003**, *342*, 64–76.
(24) van Elp, J.; Wieland, J. L.; Eskes, H.; Kuiper, P.; Sawatzky, G. A.; de Groot, F. M. F.; Turner, T. S. *Phys. Rev. B* **1991**, *44*, 6090.
(25) Kroll, T.; Knupfer, M.; Geck, J.; Hess, C.; Schwieger, T.; Krabbes, G.; Sekar, C.; Batchelor, D. R.; Berger, H.; Büchner, B. *Phys. Rev. B* **2006**, *74*, 115123.
(26) Kroll, T.; Aligia, A. A.; Sawatzky, G. A. *Phys. Rev. B* **2006**, *74*, 115124.
(27) Haverkort, M. W.; Hu, Z.; Cezar, J. C.; Burnus, T.; Hartmann, H.; Reuther, M.; Zobel, C.; Lorenz, T.; Tanaka, A.; Brookes, N. B.; Hsieh, H. H.; Lin, H.-J.; Chen, C. T.; Tjeng, L. H. *Phys. Rev. Lett.* **2006**, *97*, 176405.
(28) Evangelisti, M.; Bartolom Jongh, J.; Filoti, G. *Phys. Rev. B* **2002**, *66*, 144410.
(29) Ellis, T. S.; Park, K. T.; Hulbert, S. L.; Ulrich, M. D.; Rowe, J. E. *J. Appl. Phys.* **2004**, *95*, 982.
(30) Peisert, H.; Biswas, I.; Zhang, L.; Knupfer, M.; Hanack, M.; Dini, D.; Cook, M. J.; Chambrier, I.; Schmidt, T.; Batchelor, D.; Chassé, T. *Chem. Phys. Lett.* **2005**, *403*, 1–6.
(31) Liu, L.; Yu, J.; Viernes, N. O. L.; Moore, J. S.; Lyding, J. W. *Surf. Sci.* **2002**, *516*, 118.
(32) Upward, M. D.; Beton, P. H.; Moriarty, P. *Surf. Sci.* **1999**, *441*, 21.
(33) Shen, C.; Kahn, A. *J. Appl. Phys.* **2001**, *90*, 4549.
(34) Auerhammer, J. M.; Knupfer, M.; Peisert, H.; Fink, J. *Surf. Sci.* **2002**, *506*, 333.
(35) Molodtsova, O. V.; Knupfer, M.; Ossipyan, Yu. A.; Aristov, Yu. V. *J. Appl. Phys.* **2008**, *104*, 083704.
(36) de Groot, F. M. F.; Fuggle, J. C.; Thole, B. T.; Sawazky, G. A. *Phys. Rev. B* **1990**, *42*, 5459.
(37) Fink, J.; Nücker, N.; Pellegrin, E.; Romberg, H.; Alexander, M.; Knupfer, M. *J. Electron Spectrosc. Relat. Phenom.* **1994**, *66*, 395.
(38) de Groot, F. M. F. *Coor. Chem. Rev.* **2005**, *249*, 31.
(39) When using the formula

$$I(\theta) = \cos^2(\theta)I(0°) + \sin^2(\theta)I(90°)$$

one can derive the relations

$$I(0°) = \left(1 - \frac{\tan^2(6°)}{\tan^2(76°)}\right)^{-1} \cdot \left(\frac{I(6°)}{\cos^2(6°)} - \frac{\tan^2(6°) \cdot I(76°)}{\sin^2(76°)}\right)$$

$$I(90°) = \left(1 - \frac{\tan^2(6°)}{\tan^2(76°)}\right)^{-1} \cdot \left(\frac{I(76°)}{\sin^2(76°)} - \frac{I(6°)}{\tan^2(76°)\cos^2(6°)}\right)$$

(40) Carniato, S.; Luo, Y.; Agren, H. *Phys. Rev. B* **2001**, *63*, 085105.
(41) de Groot, F. M. F.; Fuggle, J. C.; Thole, B. T.; Sawazky, G. A. *Phys. Rev. B* **1990**, *41*, 928.
(42) van der Laan, G.; Thole, B. T.; Sawatzky, G. A.; Verdaguer, M. *Phys. Rev. B* **1988**, *37*, 6587.
(43) Zaanen, J.; Sawatzky, G. A.; Fink, J.; Speier, W.; Fuggle, J. C. *Phys. Rev. B* **1985**, *32*, 4905.
(44) Cowan, R. D. *The Theory of Atomic Structure and Spectra*; University of California Press: Berkeley, CA, 1981.
(45) van der Laan, G.; Thole, B. T. *Phys. Rev. Lett.* **1988**, *60*, 1977.
(46) Parameter set I (configuration I): $Dq = 0.23$, $Ds = 0.82$, $Dt = 0.16$; Slater−Condon parameters reduced to 65% of their Hartree−Fock value, $\zeta_i = 66$ meV (ground state), $\zeta_e = 82$ meV (excited state). Parameter set II (configuration II): $Dq = 0.28$, $Ds = 0.58$, $Dt = 0.27$; Slater−Condon parameters reduced to 70% of their Hartree−Fock value, $\zeta_i = 66$ meV (ground state), $\zeta_e = 82$ meV (excited state).

JP903001V